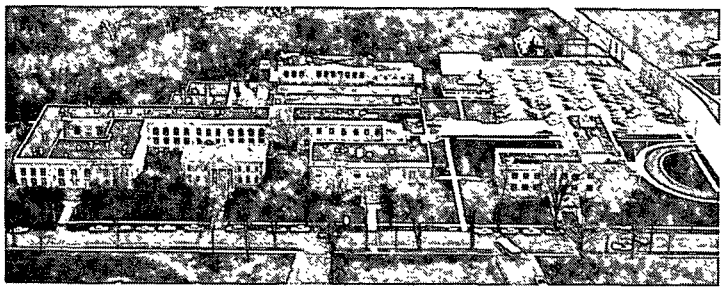

THE INSTITUTE OF PAPER CHEMISTRY, APPLETON, WISCONSIN

IPC TECHNICAL PAPER SERIES
NUMBER 282

KRAFT PULP CHLORINATION: A NEW MECHANISTIC DESCRIPTION

SEBASTIAN C. PUGLIESE, III, AND THOMAS J. McDONOUGH

MARCH, 1988

Kraft Pulp Chlorination: A New Mechanistic Description

Sebastian C. Pugliese, III, and Thomas J. McDonough

Portions of this work were used by SCP as partial fulfillment of the requirements for the Ph.D. degree at The Institute of Paper Chemistry. This manuscript will be presented at the International Pulp Bleaching Conference in Orlando, Florida on June 5-9, 1988

KRAFT PULP CHLORINATION: A NEW MECHANISTIC DESCRIPTION

Sebastian C. Pugliese, III and Thomas J. McDonough
The Institute of Paper Chemistry
1043 E. South River Street
Appleton, Wisconsin 54912

ABSTRACT

A kinetic study of kraft pulp chlorination has resulted in a novel phenomenological description of the process. The description incorporates transport of chlorine within the cell wall as the process that limits the rate of disappearance of chlorine. Characteristic features of chlorination, including the dramatic decrease in rate and the asymptotic limit to the conversion of lignin, are explained by phenomena that significantly influence intrafiber diffusion of chlorine. The rapid initial phase of chlorination is the result of unsteady diffusion of chlorine coupled with rapid chemical reactions. The reactions serve to accentuate the flux of chlorine into the cell wall by maintaining a large gradient in the concentration of chlorine. The decrease in rate, as well as the asymptotic limit to conversion, are produced by structural changes within the cell wall. They result in progressive pore closure, significantly reducing the effective diffusivity of chlorine within the cell wall and rendering certain portions of the remaining lignin macromolecule inaccessible to further reaction.

KEYWORDS

Activation Energy, Chlorination, Chlorine, Continuous Stirred Tank Reactor, Diffusion, Energy Dispersive Spectrometry, Kinetics, Mathematical Model, Rate Determining Step, Scanning Electron Microscope, Solute Exclusion Technique, Temperature

INTRODUCTION

Although it is apparently a simple process, the chlorination of kraft pulp represents a complex set of chemical and physical phenomena. These include a plethora of significant chemical reactions, including substitution, oxidation, demethylation, and electrophilic displacement (1), and several mass transport steps. Before it can react with residual lignin in the fiber wall, chlorine must be transported across several physical regions in succession: a gas-liquid interfacial film, the bulk liquid phase, a liquid film enveloping each fiber, the liquid-filled pores within the cell wall, and the polymeric constituents of the cell wall. The complexity of this system of interrelated phenomena has so far precluded a comprehensive understanding of the chlorination process.

In the study of systems such as this, it is usually assumed that the individual transport steps and chemical reaction occur in series. If one of these steps is significantly slower than the others, then it can be assumed to limit the overall rate and is referred to as the rate determining step (RDS). Knowing which step is the RDS is important because it allows the process to be modeled as if it consisted only of that step and it provides a focus for research aimed at optimizing and controlling the process.

It is also important to recognize that during any given process the identity of the RDS may change and that it may depend on conditions. In pulp chlorination, the chemical reaction is initially extremely fast and is therefore less likely to be rate limiting than at a later stage in the process when slower reactions predominate. If mixing is poor, transport of chlorine to the fiber is more likely to be the RDS than if good mixing distributes chlorine evenly throughout the pulp suspension. Good dispersion of gaseous chlorine will reduce the chances of gas-liquid mass transfer being the RDS by increasing interfacial area.

The advent of high shear mixing technology and equipment offers the possibility of improving the rate, uniformity, and control of chlorination stages by removing the obstacles inherent in poor mixing and dispersion. This narrows the range of candidates for RDS and improves the chances of successfully modeling the process. Accordingly, the present study was undertaken to identify the RDS and model the process under conditions of high turbulence and good mixing. To simplify this task we chose to confine the study to the two phase (liquid-solid) system at low consistency. This assumes that gas dispersion will be adequate to maintain sufficient chlorine in the liquid phase or that predissolved chlorine is used. In situations where neither of these conditions is met, it will be necessary to supplement the model with data on chlorine dissolution kinetics, to be obtained separately.

The type of experimental system chosen was dictated by the mixing requirement and also by the high rate of reaction of chlorine with kraft pulp. The high reaction rate makes it necessary to use a fast flow reactor to allow observation of the rate at a relatively early stage in the reaction. This, together with the need for turbulent mixing, led us to choose a continuous stirred tank reactor (CSTR) system. Under conditions of steady state operation the contents of the CSTR are uniform in composition and temperature and its use affords the ability to determine concentration-rate data pairs directly from a mass balance around the reactor. This requires only that the rates of flow of pulp and aqueous chlorine to the reactor be known, and that the concentration of chlorine at the reactor outlet be measured. Other advantages of the CSTR include the ability to achieve ideal and nonideal states of mixing by varying the impeller speed, the means to distinguish between these states, and the ability to study the reaction at lower average degrees of conversion than in the alternative plug flow reactor. Its only disadvantage is the mathematical complexity introduced at the data analysis stage by the need to account for the distribution of fiber residence times.

ASCERTAINING THE RATE DETERMINING STEP

Three likely candidates for the RDS are transport of chlorine through a liquid film enveloping each fiber, transport of chlorine within the cell wall, and chemical reaction between chlorine and lignin. A summary of hypotheses concerning the RDS from

1

previous kinetic analyses of kraft pulp chlorination is presented in Table 1. A variety of hypotheses concerning the RDS have been forwarded, although none has been universally accepted. Experimental chlorination trials have been conducted using three types of reactors: plug flow, batch, and displacement. Because the mixing conditions in these reactors were not well characterized, the results may not be applicable to well mixed systems.

Table 1. A summary of previous kinetic analyses of pulp chlorination.

Investigator	Year	Type of Reactor	Rate Determining Step
Chapnerkar (2)	1961	Batch	Chemical reaction
Rapson and Anderson (3)	1966	Displacement	Film transport
Russell (4,5)	1966	Tubular	Chemical reaction
Karter and Bobalek (6,7)	1971	Tubular	Intrafiber transport
Ackert (8,9)	1973	Batch, Displacement	Chemical reaction
Pal'vinskii (10)	1983	Batch	Chemisorption
Berry and Fleming (11)	1985	Batch	Chemical reaction

Film Transport

Rapson and Anderson (3) postulated that diffusion of a bleaching agent through an aqueous film enveloping each fiber limited the rate of bleaching. This hypothesis can be tested by determining the effect of impeller speed on the rate of disappearance of chlorine. If film diffusion is the RDS, an increase in the rate will be observed at higher speeds because of the associated reduction in film thickness. In a previous study employing a batch reactor (12) such an effect was concluded to be absent, but the hypothesis has not been tested at the short, well-controlled retention times available in a CSTR. The results of our experiments are shown in Table 2. No effect was observed over the range 1250-1550 rpm. At lower speeds, tracer studies of the fluid residence time distribution revealed the existence of macroscopic concentration gradients within the reactor, making trials at lower speeds inappropriate.

The data of Table 2 and the findings of Liebergott, et al. (12) indicate that diffusion through a liquid film enveloping individual fibers is not rate limiting for turbulent systems. This conclusion was further examined by estimating the film thicknesses present in a stirred tank reactor and comparing them to the thickness required for a film diffusion limitation to be responsible for the observed chlorination rate. With reference to trial 2 of Table 2, and assuming a pulp specific surface area of 1×10^4 cm^2 g^{-1}, the observed rate of 9×10^{-4} mol L^{-1} min^{-1} at 0.27% consistency converts to a chlorine flux of 5.55×10^{-10} mol cm^{-2} s^{-1}. According to Fick's first law of diffusion, this may be equated to the product of the diffusivity of chlorine in water, 1.24×10^{-5} cm^2 s^{-1} (13) and the gradient in chlorine concentration at the fiber surface (see Nomenclature for parameter definitions),

$$r'_{Cl} = 5.55 \times 10^{-10} \frac{\text{mol}}{\text{cm}^2\text{-s}}$$

$$= 1.24 \times 10^{-5} \frac{\text{cm}^2}{\text{s}} \frac{\Delta C_{Cl}}{d} \qquad (1)$$

Table 2. Effect of impeller speed on rate of chlorination.[a]

Trial Number	Temp., °C	Shaft Speed, rpm	Rate of Disappearance of Chlorine, mol L^{-1} min^{-1}, x 10^4
1	25.5	1250	10.0
2	26.0	1250	9.0
3	25.4	1250	8.7
4	24.1	1551	8.5
5	40.3	1300	11.0
6	40.5	1303	9.8
7	40.1	1551	11.0

[a]*Other conditions:* unbleached Klason lignin, 6.1%; fiber conc., 2.7 g L^{-1}; chlorine conc., 0.10-0.13 g L^{-1}; pH, 1.56 - 1.70; reactor space time (mean residence time), 62.6 - 67.1 s.

If film diffusion is limiting, then the resistances associated with intrafiber diffusion and chemical reaction may be neglected, and the concentration of chlorine at the fiber surface may be assumed equal to zero. Accordingly, the chlorine concentration gradient will be just equal to the bulk chlorine concentration divided by the film thickness. Solution of the above equation then gives a film thickness of 416 μm under the assumption that film transport is the RDS.

Intuition suggests that this value, being some ten times the diameter of a pulp fiber, is so large as to cast doubt upon the assumption on which its calculation is based. This conclusion is reinforced by independent estimates of the thickness of the immobilized film of fluid surrounding a fiber. Ideal flow around a solid cylinder can be used to estimate the velocity of the flow field at any

2

point around a fiber. If it is conservatively assumed that the film extends from the surface of the fiber to a point in the fluid where the local velocity is 96% of the bulk value, then the thickness of the film is determined, by application of the equation in Table 3, to be 80 μm. If the film is considered to extend only to the point where the velocity is 35% of the bulk value, its thickness is 5 μm. These calculations provide estimates of film thickness under laminar flow conditions and represent inflated values relative to the thickness that might exist in a stirred tank reactor.

In the second case, Newton's law of viscosity was used to estimate the film thickness. Typical shear stresses at the surface of a fiber were obtained from the work of Tam Doo, Kerekes, and co-workers (14,15). By laser anemometry, they determined that the shear stress at the surface of a fiber in a dynamic drainage jar was approximately 1×10^3 dyne cm^{-2} at a rotational speed of 250 rpm. The impeller radius in the CSTR is 2.94 cm; 250 rpm in this reactor corresponds to a tangential velocity of 77 cm s^{-1} at the impeller tip. This tangential velocity and the experimentally determined shear stress gave a calculated film thickness of 8 μm. By comparison, the film thickness necessary for significant film transport limitations was computed on the basis of an experimental trial conducted at a rotational speed of 1250 rpm (385 cm s^{-1}). Under these conditions the film thickness may be expected to be even lower than 8 μm and even farther removed from the value needed to account for the observed chlorination rate. These theoretical results are summarized in Table 3 and indicate that diffusion through a film is not the controlling resistance for turbulent systems.

Table 3. A comparison of estimates of film thickness in a stirred tank reactor with the film thickness necessary for film diffusion to be rate limiting.

	Equation	Calculated Film Thickness d, μm
Film thickness necessary to account for observed rate	$r'_{Cl} = j_{Cl} = D_{Cl} \frac{\Delta C_{Cl}}{d}$	416
Actual film thickness estimated from potential flow around a cylinder	$v^2 = V_\infty^2 \left(1 - \frac{2R^2}{r^2} + \frac{R^4}{r^4}\right)$	5 ($v = 0.35 V_\infty$)[a] 80 ($v = 0.96 V_\infty$)
Actual film thickness estimated from shear stress at fiber surface	$\tau_w = -\mu \frac{V_\infty}{d}$	8 (250 rpm)

[a] The calculated values are based on a cylinder radius of 21 μm.

Chemical Reaction

Chemical steps are usually much more sensitive to temperature than physical steps due to an inherently larger activation energy. Thus the influence of temperature on the observed rate of conversion can help to distinguish between chemical and physical processes as rate limiting. A series of eleven chlorination trials was therefore conducted in the CSTR, with temperatures varying from 23°C to 48°C at a space time of 78 s. The Arrhenius relationship was used to compute an activation energy of 2 kcal mol^{-1} (Fig. 1). This process was repeated for a series of six chlorination trials conducted at a space time of 33 s. The resulting activation energy was 1.4 kcal mol^{-1}. Both values are very low by comparison with the values of 20-35 kcal mol^{-1} that are usual for chemical reactions, and are indicative of a physical RDS.

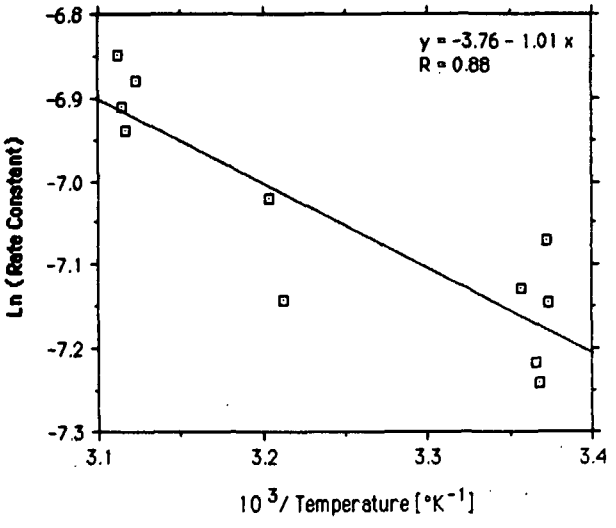

Fig. 1. A plot of the logarithm of the rate constant vs. the reciprocal of temperature for CSTR runs. Chlorination conditions: unbleached Klason lignin, 6.2%; fiber conc., 2.60 ± 0.02 g L^{-1}; chlorine conc., 0.15 ± 0.02 g/L; pH, 1.5 ± 0.1; shaft speed, 1360 ± 20 rpm; space time, 78 ± 3 s; temperature was varied from 23°C to 48°C.

Support for this conclusion was obtained by calculating activation energies from published data. The results of these calculations are presented in Table 4. The activation energies are consistently low and are observed at a variety of contact times; there appears to be no shift in the nature of the controlling resistance within the examined time frame.

Intrafiber Transport

Scanning transmission electron microscopy and energy dispersive spectrometry (STEM-EDS) were used to analyze the radial penetration of chlorine into fibers that had contacted chlorine water for various times. In this analysis, an x-ray spectrum is obtained at discrete points across the cell wall. A specific peak in this spectrum is characteristic of chlorine and can be used to determine the local concentration of chlorine. Figure 2 depicts three profiles resulting from a preliminary experiment in which fibers were exposed to chlorine water at a concentration of 2.0 g Cl_2 L^{-1}. It appears that a gradient in chlorine content, present for fibers that had contacted chlorine for ten seconds, diminishes at longer contact times. This behavior was verified statistically by linear regression (Table 5). The tabulated values for each of the slopes include the mean and the 95% confidence limits.

3

For fibers that had not contacted chlorine water or had contacted chlorine water for thirty seconds, the interval between the confidence limits includes zero. Thus the gradient is not statistically significant. The gradient is statistically significant for fibers that had contacted chlorine for ten seconds as the interval between the confidence limits does not contain zero. These results indicate that the time required for transport of chlorine from the exterior wall to the lumen, under quiescent conditions, is of the order of ten to twenty seconds and is large compared to the time anticipated to be necessary for intrinsic chemical reaction.

Table 4. Activation energies computed from published data using the Arrhenius relationship. A simple rate law of the form r = k [Chlorine] was assumed.

Reactor Type	Contact Time, s	Lignin Conversion	E_a, kcal mol^{-1}	Reference
Displacement	15	0.41	3.6	(8)
Displacement	30	0.52	3.6	(8)
Batch	45	0.62	7.0	(8)
Batch	90	0.66	2.2	(8)
Batch	150	0.61	2.0	(2)
Batch	600	0.74	3.4	(2)

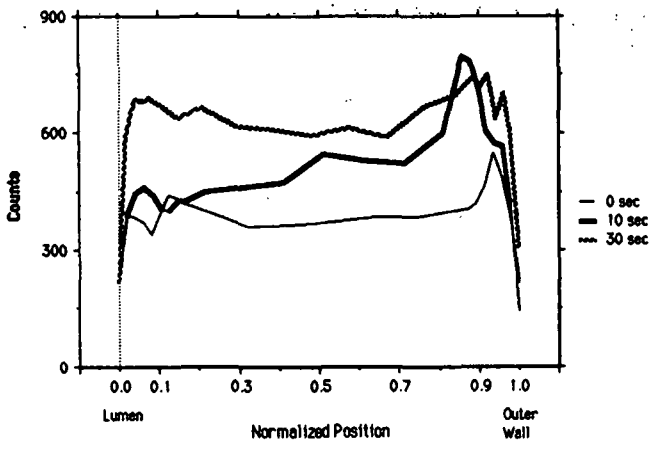

Fig. 2. Counts representing chlorine content as a function of normalized position from the lumen to the outer wall. Each profile represents the average of three or more scans. Each of the scans was determined using a cross section obtained from a different fiber.

The Weisz-Prater criterion (16), F in Eq. (2), represents the ratio of the rates of intrinsic chemical reaction and intraparticle diffusion. It has been proposed as a basis for determining whether a given system is chemical reaction or mass transfer controlled. Values much smaller than one indicate reaction control, whereas larger ones indicate intraparticle diffusion control.

$$F = \frac{(r_v)_{obs}\, L^2}{D_e\, C_s} \qquad (2)$$

Table 5. Slopes from linear regression of profiles obtained by STEM-EDS.

Contact Time, s	Slope, Mean ± 95% Confidence Limits
0	33 ± 109
10	354 ± 140
30	57 ± 140

Kinetic data published by Liebergott, et al. (12) were used to compute this ratio. The observed rate of reaction was obtained by differentiating concentration-time data pairs and converting to the appropriate units. Because film diffusion limitations are assumed to be negligible for this analysis, the concentration of chlorine at the surface of the fiber was equated to the concentration of chlorine in the bulk liquid phase. The cell wall thickness was assumed to be 4 μm.

The effective diffusivity of chlorine within the cell wall represents the most difficult parameter to estimate for this calculation. The binary diffusivity for chlorine and water was calculated to be 1.24×10^{-5} cm^2 s^{-1} using a published correlation (13). This value, however, is inappropriate for characterizing diffusion of chlorine within the cell wall. Both the pore structure and the polymeric constituents of the cell wall may be expected to significantly retard intrafiber diffusion of chlorine.

One mode of transport within the cell wall involves diffusion of chlorine through an established pore structure. The magnitude of any increased resistance to diffusion is largely dependent on pore diameter. Pore diameters in kraft fibers range from 8 Å to 300 Å (17). Thus resistance to diffusion can be expected to vary considerably. Several factors are thought to adversely affect diffusion within a porous substrate (18-20). The diffusivity characterizing diffusion in pores approximating the diameter of the solute in size may be two orders of magnitude less than the bulk diffusivity (20).

In addition to transport through an established pore structure, diffusion of chlorine through the polymeric constituents of the cell wall must be considered. This mode of transport will predominate if the system of pores is not continuous. Solvent-polymer systems of interest to the plastics industry have been studied in this respect (21). By analogy with them, the diffusivity of chlorine

4

within the polymeric constituents of the cell wall may be estimated to be several orders of magnitude less than the bulk diffusivity of chlorine in water.

In a study of the diffusion of water through cellophane (22), the effective diffusivity was determined to be 4 x 10^{-9} cm^2 s^{-1}. Although there are differences between the behavior of molecular chlorine and water as solutes, this system serves to model some of the physical phenomena associated with diffusion of chlorine through the cell wall.

Because the influence of these physical phenomena on intrafiber diffusion of chlorine is difficult to quantify, calculations of the Weisz-Prater criterion were based on four assumed effective diffusivities. The results are presented in Table 6. For an effective diffusivity of the magnitude of the bulk diffusivity, 10^{-5} cm^2 s^{-1}, the Weisz-Prater criterion takes on values much less than one. As described above, however, this value is inappropriate for characterizing diffusion of chlorine within the cell wall. For an assumed effective diffusivity of 10^{-9} cm^2 s^{-1}, a value close to that observed for the diffusion of water through cellophane (22), intrafiber diffusion is the RDS in the earlier stages of the reaction. At longer contact times, the Weisz-Prater criterion decreases. This results from a decrease in the observed rate of reaction and assumes that the effective diffusivity is time invariant. This assumption may not be valid in view of the chemical and physical changes that occur within the cell wall as reaction proceeds.

Table 6. Calculations of the Weisz-Prater criterion based on published rates of disappearance of chlorine (12).

Contact Time, min	Effective Diffusivity in Cell Wall, cm^2 s^{-1}			
	10^{-5}	10^{-7}	10^{-9}	10^{-11}
0.2	0.01	1.4	142.9	14290
1.0	<0.01	0.15	14.8	1480
5.0	<0.01	0.02	2.4	240
30.0	<0.01	0.01	1.1	110

Chlorination conditions: consistency, 2%; temperature, 20°C; 8% chlorine on OD fiber.

Analysis of Published Mathematical Models

To gain further insight into the nature of the factors controlling chlorination, four mathematical models were evaluated for their ability to correlate both published data and data from the present study. The ability to predict two well-known characteristics of pulp chlorination - the dramatic decrease in rate and the asymptotic limit to the conversion of lignin - were major criteria in evaluating the models.

The unreacted shrinking core (USC) model (23) assumes that intrinsic chemical reaction occurs at a well defined interface within a solid particle. This interface divides the outer product layer from the unreacted core and advances inward from the surface of the particle as the unreacted core shrinks due to conversion of the solid reactant. Two versions of the USC model were examined, one assuming film diffusion as the RDS and one assuming intraparticle diffusion as the RDS. For each of these models, intrinsic chemical reaction is described by a rate law that is first order with respect to chlorine. The fiber itself is modeled as a flat plate with reaction occurring at both faces.

Two models presented by Ackert (8) assuming intrinsic chemical reaction as the RDS were also analyzed. One model is a simple rate law that is second order with respect to lignin and a fractional order with respect to chlorine. The second, which in fact accurately correlated his data, incorporates two parallel reactions that are first order with respect to lignin. One of these proceeds at a rapid rate and the other is slow.

The ability of each of these models to correlate published data is depicted in Fig. 3. The reference data were obtained in a plug flow reactor (PFR) (6,7). Predictions by the USC model incorporating film diffusion as the primary resistance were based on a film thickness of 30 μm. Despite the large assumed thickness, the model predicts conversions that are greater than those found experimentally. The USC model incorporating intrafiber diffusion as the RDS assumes an effective diffusivity of 10^{-7} cm^2 s^{-1}. This value is conservative in that it recognizes the increased resistance posed by diffusion within pores but ignores diffusion through the polymeric constituents of the cell wall which would lower the estimate by several orders of magnitude. Despite the conservative estimate, the model adequately predicts the experimental conversions found at short residence times. Both versions of the USC model incorrectly predict complete conversion of lignin at some finite time.

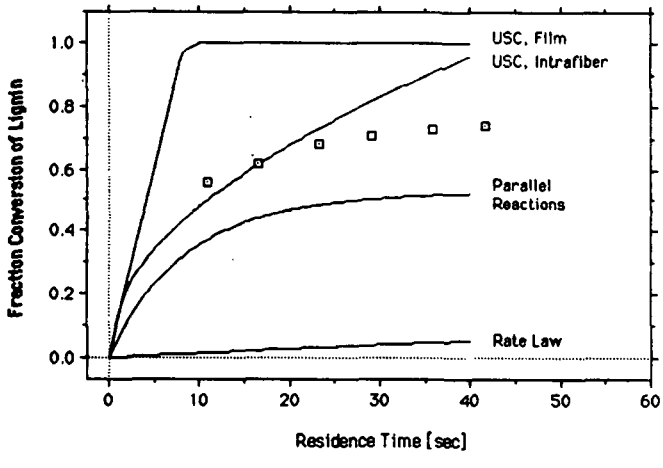

Fig. 3. A comparison of the fraction conversions of lignin determined experimentally in a plug flow reactor (6,7) (data points) with those predicted by selected models. Experimental conditions: unbleached Kraft lignin, 5.4%; consistency, 0.2%; chlorine concn., 0.5 g L^{-1}; pH, 2.0; temperature, 26°C.

5

The rate law proposed by Ackert grossly underpredicts the experimental conversions. The model involving parallel first order reactions predicts the rapidly diminishing rate but incorrectly predicts their magnitude. Both models required introduction of an empirical factor to characterize the asymptotic limit to conversion.

The models were also tested for their ability to correlate data obtained in the CSTR. In contrast to the PFR, a distribution of fiber residence times characterizes the CSTR. Thus the exit age distribution of a CSTR was incorporated into both versions of the USC model. The resulting model predictions are depicted in Fig. 4 and are based on the parameter values selected for analysis of PFR data. The USC model incorporating film diffusion as the controlling resistance predicts conversions that are greater than those found experimentally. The model incorporating intrafiber diffusion as the rate limiting step satisfactorily correlates the experimental data. As stated earlier, these models are unacceptable in that they predict complete conversion of lignin at some finite time. The preceding conclusions for models assuming chemical reaction as the controlling resistance are relevant here. The model incorporating parallel first order reactions appears to more accurately correlate the CSTR data compared to the PFR data. This is simply a result of the lower conversions found in the CSTR; the model predictions are nearly equivalent for the two data sets.

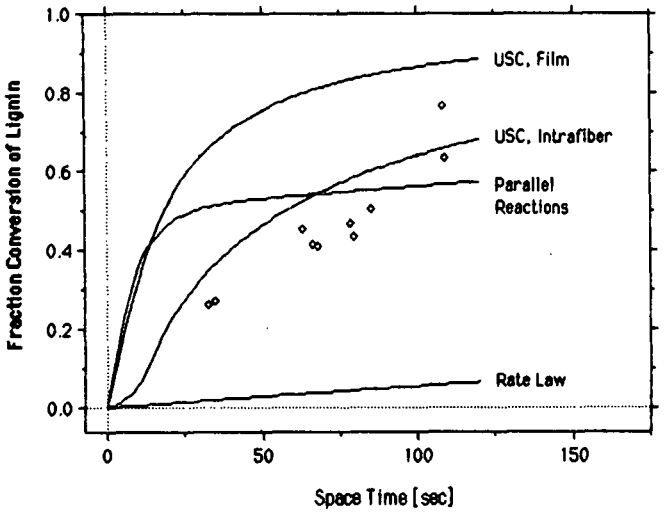

Fig. 4. A comparison of the fraction conversions of lignin determined from CSTR experiments (data points) with those predicted by selected models. The rates of disappearance of chlorine determined in the CSTR were used to calculate the fraction conversion of lignin by assuming that one gram of chlorine is consumed for each gram of lignin rendered soluble in the subsequent extraction stage. Experimental conditions: unbleached Klason lignin, 5.5 ± 0.9%; fiber conc. 2.7 ± 0.5 g L^{-1}; chlorine conc., 0.15 ± 0.05 g L^{-1}; pH, 1.6 ± 0.25; temperature, 25 ± 1°C.

A NEW MECHANISTIC DESCRIPTION

The preceding experimental and theoretical analyses and their compatibility with the hypothesized rate controlling steps are summarized in Table 7. The activation energies determined in this study and other published investigations are low and indicative of a physical RDS. Film transport does not appear to be the primary resistance, however, as increasing the impeller speed did not influence the rate and the film thicknesses estimated to exist in a stirred tank reactor were not of the magnitude necessary for significant limitations. The other analyses are supportive of intrafiber mass transport as the controlling resistance.

Table 7. Compatibility of assumed rate limiting steps with experimental and theoretical analyses. This matrix applies to chlorination in a turbulent system at low consistencies.

	Limiting Step		
Analysis	Film Diffusion	Chemical Reaction	Intrafiber Diffusion
1. Low activation energy	+	-	+
2. Gradient in chlorine content (STEM-EDS)	-	-	+
3. Influence of impeller speed	-	+	+
4. Calculated film thickness	-	+	+
5. Weisz-Prater criterion	-	-	+

A plus sign indicates that the hypothesized limiting step is compatible with the observed behavior. A negative sign indicates that it is not.

The preceding information has led to the formation of a new hypothesis governing chlorination under turbulent conditions and at low consistencies (< 3%). The rapid early phase of delignification is characterized by unsteady diffusion of chlorine into the fiber coupled with rapid chemical reactions. These reactions act as a sink and serve to maintain a large gradient in the concentration of chlorine, thereby dramatically accentuating the flux. This situation produces the extremely rapid consumption of chlorine that characterizes the initial seconds of chlorination. Substitution reactions immobilize chlorine as it diffuses into the cell wall, reducing the apparent diffusion coefficent by several orders of magnitude. Thus a gradient in chlorine content is observed across an extremely thin cell wall (≈ 4 μm) after a relatively long period of time (10 sec).

The decrease in rate, as well as the asymptotic limit to conversion, are accounted for by postulating structural changes within the cell wall. The lignin macromolecule is significantly altered

by reaction through the breaking of interunit bonds. Lignin, and perhaps other cell wall constituents, assume more degrees of freedom and are able to occupy more volume within the cell wall. This results in progressive pore closure, significantly reducing the effective diffusivity of chlorine within the cell wall and rendering certain portions of the remaining lignin macromolecule inaccessible to further reaction.

This hypothesis was quantified by adapting a model from the chemical engineering literature to characterize pulp chlorination. The grain model (24,25), depicted in Fig. 5, was selected because of recognized similarities between pulp chlorination and chemical reaction in porous catalysts. The fiber is characterized as a flat plate. Within the plate there exist individual spherical grains that are composed of a cellulose-hemicellulose-lignin matrix. Between the spherical grains is a liquid-filled void that represents the network of pores in the fiber wall. Each grain is assumed to react as described in the USC model. In order for chlorine to react with lignin, it must diffuse through the liquid-filled void to the surface of the grain, through any product layer that exists, to the surface of the unreacted core. As reaction proceeds, the product layer increases in volume as the unreacted core shrinks toward the center of the grain. If the molar volume of the solid product is greater than the molar volume of the solid reactant, then the grain swells as reaction proceeds. This phenomenon causes the pores to constrict, thereby retarding diffusion in the void. The grains can swell to a point where transport through the void becomes impossible; any solid reactant remaining in the particle at this point is unconverted. Thus the model can account for incomplete conversion of the solid reactant.

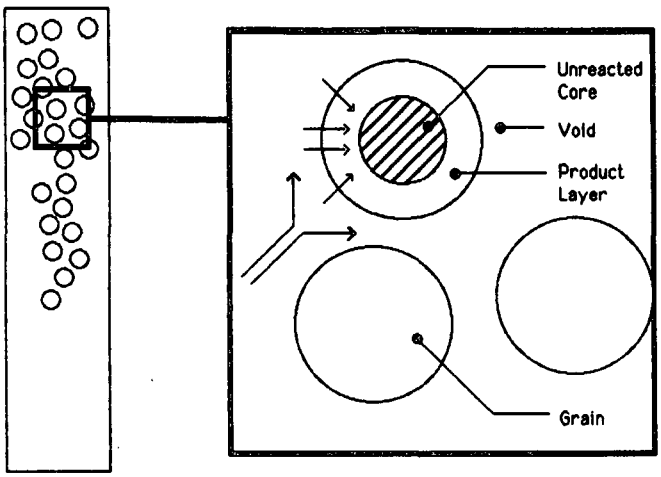

Fig. 5. A schematic of the fiber wall as represented in the grain model. The fiber wall is modeled as a flat plate. Within the plate there exist spherical grains composed of a cellulose-hemicellulose-lignin matrix. Between the grains is a liquid-filled void. Chlorine must diffuse through the void and any product layer before reacting with lignin at the surface of the unreacted core.

The modified model consists of three coupled partial differential equations and will be described in a separate publication. The three equations respectively characterize the outside radius of the spherical grains, the radius of the unreacted core, and the concentration of chlorine within the pores as a function of time and position. This information is used to compute the overall conversion of lignin for the fiber as a function of time. The exit age distribution is incorporated into the model for prediction of conversions at the outlet of a CSTR. A comparison of rates obtained in the CSTR with predictions by the grain model is presented in Fig. 6. Of the parameters that characterize the model, all but two were estimated a priori or were determined from the experiments being simulated. The effective diffusivity of chlorine within the solid grains was assumed to be 10^{-10} cm^2 s^{-1}. A relatively low value was assumed as it characterizes diffusion solely within polymeric substances. The remaining parameter characterizes the ratio between the molar volume of the product and the molar volume of the reactant. A value of 1.64 was selected to predict the rate of disappearance of chlorine for one experiment. The parameter remained fixed at this value for remaining predictions.

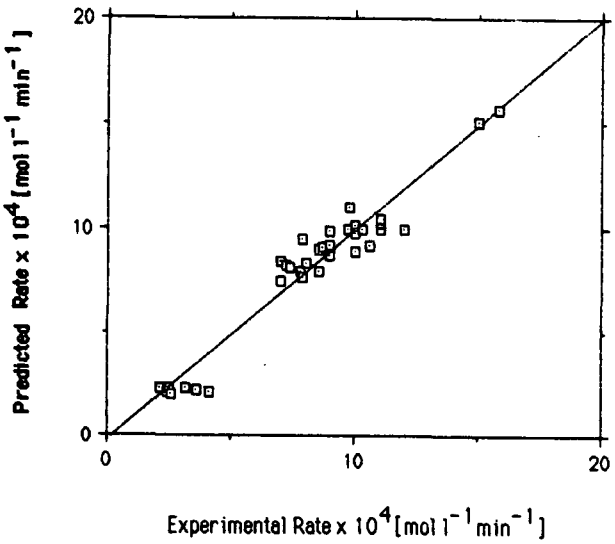

Fig. 6. Experimentally determined rates of disappearance of chlorine *vs.* rates predicted by the grain model.

Support for the hypothesis underlying this model was sought by measuring the distribution of pore sizes in the fiber wall before and after chlorination. A modified solute exclusion technique (SET) was used to determine the accessibility of the cell wall to chemical probes of varying molecular size (17,26). The probes used for this study include glucose and three different dextrans. The distributions for kraft fibers and chlorinated fibers are depicted in Fig. 7. The top panel shows the excellent reproducibility of the three pore size distributions determined for kraft fibers. Each distribution is comprised of the cumulative pore volumes determined at each of four pore diameters. The cumulative pore volume determined for a single pore diameter is the average of four replicate analyses. Thus a three-spoked symbol represents overlap of

twelve individual determinations of cumulative pore volume, four for each of the distributions depicted in the top panel. The precision of the cumulative pore volume determined using glucose is significantly less than for the values determined using the larger chemical probes. Thus little can be concluded in comparisons concerning this region of the distribution (8Å). The bottom panel depicts the pore size distributions for fibers that had been chlorinated for 60 min. The distributions indicate that there has been a reduction in the cumulative pore volume for larger pores (50-270Å). This result shows that pulp chlorination is accompanied by structural changes within the cell wall that cause pore closure. The pore size distributions for chlorinated and extracted fibers are presented in Fig. 8. The cumulative pore volume for the larger pores (50-270Å) has increased relative to the distribution for chlorinated fibers. This behavior is consistent with the removal of chlorinated lignin during the extraction stage. It appears that the total pore volume for these fibers is slightly greater than the total pore volume for untreated kraft fibers.

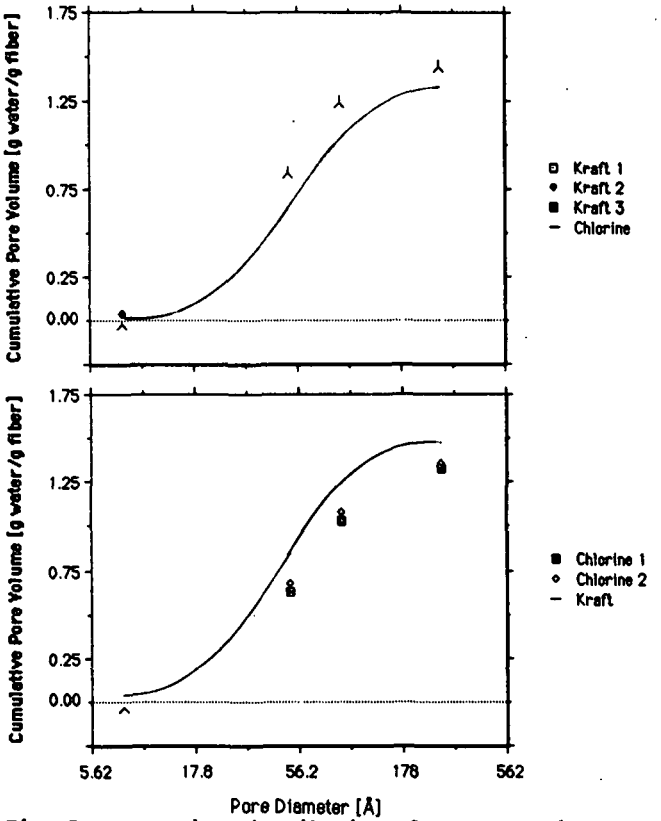

Fig. 7. Pore size distributions for untreated kraft fibers and chlorinated fibers. Each panel depicts the distributions obtained for each of these fiber types, three for kraft fibers and two for chlorinated fibers. Each distribution is comprised of cumulative pore volumes determined at each of four pore diameters. The two- and three-spoked symbols indicate overlap between two or three experimental points, respectively. Appropriate curves are drawn for comparison. Chlorination conditions: unbleached Klason lignin, 6.1%; consistency, 3%; temperature, 20-22°C; 8.1% chlorine on OD fiber; 1 hr.

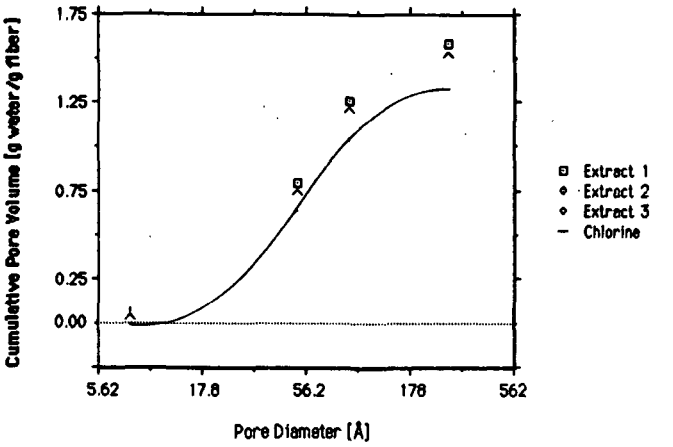

Fig. 8. Pore size distributions for chlorinated and extracted fibers. Each of the three distributions is comprised of cumulative pore volumes determined at each of four pore sizes. A curve for chlorinated fibers is drawn for comparison. The two- and three-spoked symbols indicate overlap between two or three experimental points, respectively. Chlorination conditions: unbleached Klason lignin, 6.1%; consistency, 3%; temperature, 20-22°C; 8.1% chlorine on OD fiber; 1 hr. Extraction conditions: consistency, 10%; temperature, 70°C; 4.5% NaOH on OD fiber; 1 hr.

The results of the SET experiments and the ability of the grain model to correlate experimentally determined rates provide support for our hypothesis concerning the mechanism of pulp chlorination under turbulent conditions and at low consistencies. Although the grain model is not yet in an optimized form, it satisfactorily correlates the data obtained in the CSTR. It is a phenomenologically sound model in that it predicts both the rapid decrease in the rate of reaction as well as the asymptotic limit to the conversion of lignin and therefore represents a significant advance over previous models.

EXPERIMENTAL

Chlorination Trials

Chlorination trials were conducted at low consistencies in a continuous stirred tank reactor (CSTR). The reactor consists of a hollow Teflon cylinder in a brass jacket. A diagram of the reactor and supporting apparatus is depicted in Fig. 9. An aqueous pulp slurry of the appropriate consistency was prepared in the pulp reservoir, a high density polyethylene (HDPE) 120 L rectangular tank. A centrifugal pump used to recycle the slurry and three variable-speed stirrers kept the pulp uniformly dispersed within the tank. If the trial was to be conducted at a temperature other than ambient, a quartz heater within the pulp reservoir and a water bath used to circulate heated water to the reactor's jacket were activated. Chlorine water was prepared by passing chlorine gas through a column of 0.3N HCl for the appropriate time. The

8

concentration of chlorine within the reservoir was then determined iodometrically. An experiment was initiated by starting the flows of pulp slurry and chlorine water to the CSTR. The desired impeller speed within the reactor was selected by adjusting a variable-speed stirrer. After steady state operation was achieved, samples were taken at the reactor outlet every 3-4 min and quenched immediately in a solution of potassium iodide pending titration to determine their chlorine content. The rate of disappearance of chlorine was then computed from Eq. (3), a mass balance over the reactor.

$$\tau = \frac{V_R}{V_o} = \frac{C_{Cl,in} - C_{Cl,out}}{-r_{Cl}} \qquad (3)$$

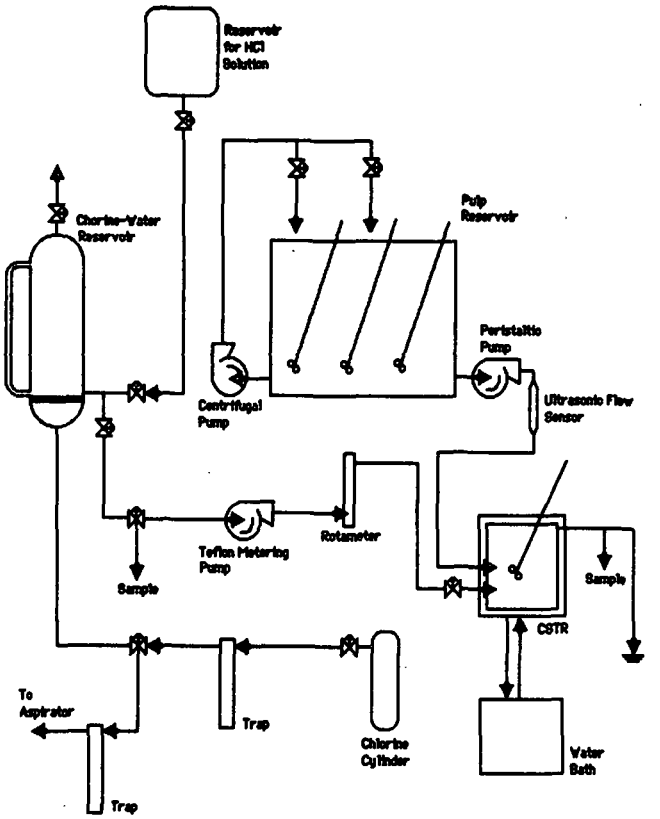

Fig. 9. Flow diagram of chlorination apparatus.

Scanning Transmission Electron Microscopy-Energy Dispersive Spectrometry

A swatch of approximately ten fibers was attached to a length of plastic capillary tubing using a polyethylene glycol (m.p. 85°C). Prior to exposure to chlorine water, fibers were immersed in distilled water for five minutes. Each swatch of fibers was then immersed in approximately 400 mL of quiescent chlorine water for different lengths of time. Upon withdrawal from the chlorine water, the fibers were placed in 500 mL of distilled water for an additional five minutes. The treated fibers were then dried by making a series of liquid exchanges involving acetone. The dried fibers were embedded using Spurr's resin and sectioned using a Sorvall Porter-Blum MT2-B ultramicrotome. STEM-EDS linescans of the resulting sections were performed with a Jeol-100CX scanning transmission electron microscope with a Tracor Northern TN-2000 energy dispersive spectrometer.

Solute Exclusion Technique

The basic technique as outlined by Stone and Scallan (26) was conducted with two modifications. First, experiments were conducted using solutions at low temperatures (2-4°C) in order to minimize diffusion of chlorolignin out of the fibers during analysis. Although the low temperature was necessary only for chlorinated pulp, all analyses were conducted at this temperature to be consistent. Procedural modifications involved prechilling both the pulp to be analyzed and solutions of the appropriate chemical probes (glucose and dextrans of various molecular weights). To determine the influence of temperature on the analysis, experiments were conducted to determine the pore size distributions of untreated kraft fibers at ambient temperature (20-22°C) and at low temperatures (2-4°C). The resulting distributions indicated that temperature had no effect.

A second modification involved the equation used to calculate the inaccessible water, or pore volume, for a particular chemical probe. The original equation is presented as Eq. (4); parameter definitions and their accompanying units are provided as they are an integral part of the analysis that follows.

$$M_i = \frac{w + q}{p} - \left(\frac{w}{p} \times \frac{c_i}{c_f}\right) \qquad (4)$$

M_i = inaccessible water, g water/g OD fiber
w = mass of added solution, g
p = mass of dry sample, g
q = mass of water in sample, g
c_i = concentration of stock solution, g solute/g solution
c_f = concentration of sample solution, g solute/g solution

To calculate the inaccessible water of a sample, Stone and Scallan assumed equality between the ratio of concentrations in Eq. (4) and the ratio of rotations determined using a polarimeter. An examination of Eq. (5), however, indicates that the units of concentration are not consistent between these two equations.

$$c = \frac{100\ a}{b\ [a]} \qquad (5)$$

a = observed rotation, °
$[a]$ = specific rotation, °
c = concentration of solution, g solute/100 mL solution
b = cell length, dm

The density of both the sample solution and the stock solution must be accounted for, as in Eq. (6). This equation was used to determine inaccessible water throughout this investigation.

9

$$M_i = \frac{w + q}{p} - \left(\frac{w}{p} \times \frac{a_i\ \rho_f}{a_f\ \rho_i}\right) \qquad (6)$$

ACKNOWLEDGMENT

A portion of a thesis submitted by S. P. in partial fulfillment of the requirements of The Institute of Paper Chemistry for the degree of Doctor of Philosophy from Lawrence University, Appleton, Wisconsin.

The authors gratefully acknowledge the assistance of Dr. J. Cameron and Dr. P. Parker. Thanks are also extended to M. Filz, P. Van Rossum, and G. Winkler for fabrication of the CSTR and to E. Foxgrover for analyses involving STEM-EDS.

NOMENCLATURE

a_i	=	rotation of stock solution, °
a_f	=	rotation of sample solution, °
C_{cl}	=	chlorine concentration, mol cm^{-3}
$C_{cl,in}$	=	chlorine concentration determined at CSTR inlet, mol cm^{-3}
$C_{cl,out}$	=	chlorine concentration determined at CSTR outlet, mol cm^{-3}
C_s	=	concentration of fluid reactant at particle surface, mol cm^{-3}
d	=	thickness of film, cm
D_{cl}	=	binary diffusivity for chlorine and water, $cm^2\ s^{-1}$
D_e	=	effective diffusivity, $cm^2\ s^{-1}$
F	=	Weisz-Prater criterion, dimensionless
j_{cl}	=	mass flux of chlorine, mol $cm^{-2}\ s^{-1}$
L	=	1/2 thickness of cell wall, cm
M_i	=	inaccessible water, g water g^{-1} OD fiber
p	=	mass of dry fiber sample, g
q	=	mass of water associated with wet sample, g
r	=	radial position from center of solid cylinder, cm
r_{cl}	=	rate of disappearance of chlorine per unit volume, mol $cm^{-3}\ s^{-1}$
r'_{cl}	=	rate of disappearance of chlorine per unit area, mol $cm^{-2}\ s^{-1}$
$(r_v)_{obs}$	=	observed rate per unit volume of particle, mol $cm^{-3}\ s^{-1}$
R	=	radius of solid cylinder, cm
t	=	time, s
v	=	local velocity in flow field, cm s^{-1}
V_R	=	volume of CSTR, cm^3
V_∞	=	velocity of bulk fluid, cm s^{-1}
V_o	=	volumetric flow rate at CSTR outlet, $cm^3\ s^{-1}$
w	=	mass of added solution (chemical probe), g
z	=	Cartesian coordinate, cm
μ	=	viscosity, g $cm^{-1}\ s^{-1}$
ρ_i	=	density of stock solution, g cm^{-3}
ρ_f	=	density of sample solution, g cm^{-3}
τ	=	space time, s
τ_w	=	shear stress, dyne cm^{-2}

LITERATURE CITED

1. Dence, C. and Annergren, G., in "The Bleaching of Pulp," ed. by R. P. Singh, 3rd ed., TAPPI Press, Atlanta, Georgia, 1979, pp. 33-36.

2. Chapnerkar, V., "A Kinetic Study of the Chlorination of Unbleached Kraft Pulp," Doctoral Dissertation, University of Florida, Gainsville, Florida, 1961.

3. Rapson, W. and Anderson, C., "Dynamic Bleaching: Continuous Movement of Pulp Through Liquor Increases Bleaching Rate," Tappi **49**(8): 329 (1966).

4. Russell, N., "A Study of the Initial Phase of the Aqueous Chlorination of Kraft Pulp Meals," Doctoral Dissertation, The Institute of Paper Chemistry, Appleton, Wisconsin, 1966.

5. Russell, N., "The Initial Phase of the Aqueous Chlorination of Kraft Pulp Meals," Tappi **49**(9): 418 (1966).

6. Karter, E., "The Role of Physico-Chemical Rate Phenomena in Wood Pulp Chlorination," Doctoral Dissertation, University of Maine, Orono, Maine, 1968.

7. Karter, E. and Bobalek, E., "The Role of Physico-Chemical Rate Phenomena in Wood Pulp Chlorination," Tappi **54**(11): 1882 (1971).

8. Ackert, J., "Kraft Pulp Chlorination Kinetics," Doctoral Dissertation, University of Idaho, Moscow, Idaho, 1973.

9. Ackert, J., Koch, D., and Edwards, L., "Displacement Chlorination of Kraft Pulps - An Experimental Study and Comparison of Models," Tappi **58**(10): 141 (1975).

10. Pal'vinskii, Y., "Kinetics of Pulp Chlorination," Mezhvuz. Sb. Nauchn. Tr., Khim. Tekhnol. Drev. Tsellyul., Leningrad, 1983, pp. 53-56.

11. Berry, R. and Fleming, B., "Why Does Chlorination and Extraction Fail to Delignify Unbleached Kraft Pulp Completely?," International Symposium on Wood and Pulping Chemistry (Vancouver), 26-30 August, 1985, pp. 71-78.

12. Liebergott, N., Trinh, D., Poirier, N., and Crotogino, R., "Chlorination of Pulp - The Effect of Mixing Intensity, Chlorine Concentration, and Reaction Temperature. Part I: Chlorine Water-Pulp System," Pulping Conference Proceedings (San Fransisco), 12-14 November, 1984, pp. 359-368 (Book 2).

13. Siddiqi, M. and Lucas, K., "Correlations for Prediction of Diffusion in Liquids," Can. J. Chem. Eng. **64**(5): 839 (1986).

14. Tam Doo, P., Kerekes, R., and Pelton, R., "Estimates of Maximum Hydrodynamic Shear Stresses on Fibre Surfaces in Papermaking," J. Pulp Paper Sci. **10**(4): J80 (1984).

15. Kerekes, R. and Garner, R., "Measurement of Turbulence in Pulp Suspensions by Laser Anemometry," Trans. Tech. Sect., J. Pulp Paper Sci. 8(3): TR53 (1982).

10

16. Froment, G. and Bischoff, K., "Chemical Reactor Analysis and Design," John Wiley & Sons, New York, 1979, pp. 190-197.

17. Stone, J. and Scallan, A., "A Structural Model for the Cell Wall of Water Swollen Wood Pulp Fibres Based on their Accessibility to Macromolecules," Cellulose Chem. Technol. 2(3): 343 (1968).

18. Cussler, E., "Diffusion: Mass Transfer in Fluid Systems," Cambridge University Press, Cambridge, 1984, pg. 189.

19. Israelachvili, J., "Measurement of the Viscosity of Liquids in Very Thin Films," J. Colloid Interface Sci. 110(1): 263 (1986).

20. Ternan, M., "The Diffusion of Liquids in Pores," Can. J. Chem. Eng. 65(2): 244 (1987).

21. Duda, J., Vrentas, J., Ju, S., and Liu, H., "Prediction of Diffusion Coefficients for Polymer-Solvent Systems," AIChE Journal 28(2): 279 (1982).

22. Doty, P., Aiken, W., and Mark, H., "Water Vapor Permeability of Organic Films," Ind. Eng. Chem., Anal. Ed. 16(11): 686 (1944).

23. Levenspiel, O., "Chemical Reaction Engineering," 2nd ed., John Wiley & Sons, New York, 1972, pp. 361-368.

24. Hartman, M. and Coughlin, R., "Reaction of Sulfur Dioxide with Limestone and the Grain Model," AIChE J. 22(3): 490 (1976).

25. Hartman, M. and Coughlin, R., "Reaction of Sulfur Dioxide with Limestone and the Influence of Pore Structure," Ind. Eng. Chem., Process Des. Develop. 13(3): 248 (1974).

26. Stone, J. and Scallan, A., "The Effect of Component Removal Upon the Porous Structure of the Cell Wall of Wood. II. Swelling in Water and the Fiber Saturation Point," Tappi 50(10): 496 (1967).

11